Published in final edited form as:
Neuropathol Appl Neurobiol. 2012 April ; 38(2): 162–174. doi:10.1111/j.1365-2990.2011.01200.x.

S100β as a novel and accessible indicator for the presence of monocyte-driven encephalitis in AIDS

Nicole A. Renner, **Rachel K. Redmann**, **Terri Moroney-Rasmussen**, **Hope A. Sansing**, **Pyone Pyone Aye**, **Peter J. Didier**, **Andrew A. Lackner**, and **Andrew G. MacLean***
Division of Comparative Pathology, Tulane National Primate Research Center, Tulane School of Medicine, Covington, LA 70433

Abstract

Aims—The pathogenesis of HIV/SIV encephalitis (HIVE/SIVE) remains incompletely understood, but is associated with alterations in the blood brain barrier. Heretofore, it has not been possible to easily determine if an individual has HIVE/SIVE before post mortem examination.

Methods—We have examined serum levels of the astroglial protein S100β in SIV-infected macaques and show that it can be used to determine which animals will have SIVE. We also checked for correlations with inflammatory markers such as CCL2/ MCP-1, IL-6 and C Reactive Protein (CRP).

Results—We also found that increased S100β protein in serum correlated with decreased expression of the tight junction protein zonula occludens-1 on brain microvessels. Further, the decrease in zonula occludens-1 expression was spatially related to SIVE lesions and perivascular deposition of plasma fibrinogen. There was no correlation between encephalitis and plasma levels of IL-6, MCP-1/CCL2 or CRP.

Conclusions—Together these data indicate that SIVE lesions are associated with vascular leakage that can be monitored by S100β protein in the periphery. The ability to simply monitor the development of SIVE will greatly facilitate studies of the neuropathogenesis of AIDS.

Introduction

In animals infected with pathogenic strains of simian immunodeficiency virus (SIV), such as SIVmac239 and SIVmac251, the virus can be consistently found in the central nervous system (CNS) within 10 to 14 days of infection at the time of peak viremia. This also appears to be true in human immunodeficiency virus (HIV)-infected humans, but the number of cases examined during peak viremia is very small [1, 2]. In SIV-infected macaques at this early time point, endothelial cells of the blood-brain barrier (BBB) are activated and integrity of the BBB is compromised [3]. As viral loads decline toward set point at roughly two months post infection the endothelial activation subsides and BBB integrity is largely restored [1, 4–6]. However, in the terminal phases of disease, viral loads rise and approximately one third of the animals develop SIV encephalitis which is associated with breakdown of the BBB.

The exact mechanisms of BBB disruption are unclear, but it is known that numerous resident and transitory cell populations in the CNS can be infected, with CD14-positive perivascular macrophages being the primary, productively-infected cell type [7–15]. Nervous system manifestations associated with HIV infection of humans or SIV infection of

*Corresponding author. Phone: (985) 871 6489, Fax: (985) 871 6390, amaclean@tulane.edu.

rhesus macaques include an encephalitis (SIV or HIV encephalitis, SIVE/HIVE) characterized by astrocytic and microglial activation and scattered perivascular aggregates of mononuclear cells and multinucleated giant cells. These perivascular lesions contain large numbers of HIV/SIV-infected cells, the majority of which are monocyte/macrophages. The presence of cells productively-infected with SIV/HIV in the parenchyma has been shown to induce a response in astrocytes [16–19] which in turn may lead to decreased tight junction protein expression and a leaky BBB [5, 20–29].

If the integrity of the BBB is compromised, then proteins normally confined within the CNS, such as S100β [30], could end up in the circulation in increased amounts [31–35]. Thus an S100β ELISA has been used in humans undergoing cardiac bypass surgery to monitor changes in BBB function in real time [32, 36]. Since HIV/SIV infection is known to cause encephalitis and to degrade the integrity of the BBB, we sought to examine the utility of serum levels of S100β to indicate the presence of SIVE. We correlated serum levels of S100β with tissue-based studies examining both BBB structure and function. The structure of the BBB was assessed by measuring loss of expression of the tight junction protein zonula occludens-1 (ZO-1) [3, 24, 37], while functional integrity of the BBB was assessed by examining leakage of fibrinogen into the brain parenchyma. We found that animals with increased S100β in serum also had decreased expression of ZO-1 on brain microvessels spatially related to SIVE lesions and perivascular leakage of the plasma protein fibrinogen. In contrast to S100β, there was no correlation between circulating levels of IL-6, CCL2 or CRP with SIVE. Together, these data indicate that SIVE lesions are associated with vascular leakage that can be monitored by S100β protein in the periphery.

Materials and Methods

Animals, tissues and virus

Tissue from 11 uninfected and 22 SIV-infected Indian-origin rhesus macaques (*Macaca mulatta*) were used for this study, for a total of 33 animals (Table 1). All of the animals with SIV were infected intravenously with 50 ng p27 of either SIVmac239 or SIVmac251, as specified in Table 1.

All monkeys were housed at the Tulane National Primate Research Center in accordance with the standards of the Association for Assessment and Accreditation of Laboratory Animal Care and the "Guide for the Care and Use of Laboratory Animals" prepared by the National Research Council, National Academic Press, Washington, DC). The Tulane Institutional Animal Care and Use Committee approved all studies.

The TNPRC maintains a database with clinical data for all non-human primates. This database includes body weight data from each time an animal receives a physical exam. All animals assigned to projects receive at least one physical exam per month. Body weight data were assessed to determine if loss of body mass had an independent impact on changes in serum S100β levels.

All animals were humanely euthanized with an intravenous overdose of pentobarbital and tissues collected at necropsy. A routine set of brain tissues including: occipital lobe, meninges, frontal lobe, parietal lobe, thalamus, subcortical white matter, choroid plexus, cerebellum, brainstem, hippocampus, and basal ganglia were collected. Tissues were fixed in 10% neutral buffered formalin, embedded in paraffin, and sectioned at 6 μm.

Histopathology—Multiple histological sections from different regions of brain were stained with hematoxylin and eosin. The sections were examined in a blinded fashion by the Chief of Pathology, and inflammatory foci enumerated at low power. The area of each

section was determined by point counting to determine the total area of the section with a 3.3 mm overlay grid [38]. Lesions per mm^2 for each animal were calculated and used in graphical comparisons and statistical tests. Inflammatory lesions in other tissues, including lung, liver, heart, salivary gland, trachea, kidney, sciatic nerve, lymph nodes, bone marrow spleen, small intestine, colon, jejunum, muscle, skin and reproductive organs were also evaluated for lesion intensity on a scale of 0 to 4 and frequency among the groups of animals by a pathologist and recorded.

S100β determinations—Blood was obtained by venipuncture from each animal at the time of euthanasia using a standard Vacutainer® (Becton Dickinson, Franklin Lakes, NJ) clot tube and the serum separated, aliquoted, labeled and stored at −80°C until ready for use. Each aliquot underwent a single freeze-thaw cycle. We used the same commercially available ELISA kit used to evaluate S100β in humans [31], as specified by the manufacturer (Diasorin, MN). The ELISA assays were performed in a blinded fashion. Values for S100β were plotted using Excel and SPSS statistical software (Chicago, IL), and results were compared using one-way ANOVA with Tukey's post-hoc test, and Pearson correlation.

To determine if loss of body mass might be related to the increased S100β protein in serum, we determined the changes in body weight of macaques from before they were infected with SIV and throughout disease progression. These data were tabulated and correlated against the level of S100β protein as determined by ELISA. We also determined correlations of S100β protein in serum with peak and terminal viral loads.

Determination of inflammatory protein concentrations—The concentration of IL-6 or MCP-1/CCL2 and C-Reactive Protein (CRP) was determined from plasma samples taken on the animals' day of necropsy. IL-6 and CCL2 were measured using a non-human primate-specific cytokine bead array kit from Millipore (Billerica, Massachusetts), per manufacturer's instructions. Quantification of CRP was performed using an Olympus AU400e Chemistry Analyzer. Data were analyzed using the Kruzkal-Wallis test, with Dunn's post-test with *InStat* (La Jolla, CA).

Confocal microscopy—Formalin-fixed, paraffin-embedded tissues were sectioned at 6μm and mounted onto positively charged glass slides. Sections were baked for 1 h at 60°C, deparaffinized in xylene, and then rehydrated in graded concentrations of ethanol. Antigen retrieval was carried out for 20 min using a microwave on high power and a citrate-based antigen unmasking solution (Vector Labs, Burlingame, CA). Tissues were blocked in a 10% normal goat serum solution (GIBCO/ Invitrogen, Carlsbad, CA) for one hour at room temperature before antibodies were applied. Antibodies used for immunofluorescence studies are included in Table 2. Tissues were incubated with primary antibodies to ZO-1 (Zymed), and/or fibrinogen (Dako) overnight at 4°C, washed three times with PBS with 0.2% fish skin gelatin (PBS/FSG), and then incubated in the dark for 60 min at room temperature with secondary antibodies directly conjugated with Alexa 488 (green) or Alexa 568 (red) (Molecular Probes/Invitrogen, Carlsbad, CA). For nuclear staining, slides were incubated in TO-PRO diluted 1:1000 in PBS for 10 minutes. Sections were washed three times in PBS/FSG, coverslipped with antiquenching reagent (Molecular Probes/Invitrogen), and imaged on a Leica TCS SP II confocal microscope equipped with three lasers. Individual optical slices represent 0.2 μm, and 16 to 42 optical slices were collected at 512 × 512 pixel resolution for each section.

Quantification of ZO-1 and Fibrinogen expression

Images of non-overlapping fields were captured by confocal microscope and analyzed using ImageJ (version 1.43r, NIH). Single channel images were measured for mean intensity of ZO-1 expression. Statistics were preformed using *InStat* (La Jolla, CA); comparisons were made by Kruskal-Wallis test with Dunn's post test, and fibrinogen leakage was analyzed using Chi-squared test.

In situ hybridization

In situ hybridization for SIV RNA was performed as previously described [39]. Briefly, formalin-fixed, paraffin-embedded tissue sections were pretreated in a microwave with citrate buffer (antigen unmasking solution; Vector Laboratories, Burlingame, CA) for 20 minutes at high power according to the manufacturer's instructions. Thereafter, sections were thoroughly washed, placed in a humidified chamber and prehybridized at 45°C with hybridization buffer (containing 50% formamide with sheared salmon sperm DNA (50ng/ml) and yeast tRNA (100 ng/ml)). SIV-digoxigenin-labeled antisense riboprobes (Lofstrand Laboratories, Gaithersburg, MD) were used at a concentration of 10 ng/slide in hybridization buffer and hybridized overnight at 45°C. After hybridization, slides were washed with 2x standard saline citrate, 1x standard saline citrate, 0.1x standard saline citrate and blocking solution was applied. Fab fragments of an anti-digoxigenin antibody from sheep, conjugated with alkaline phosphatase (Roche, Penzberg, Germany), were used to detect digoxigenin-labeled probes. Controls included matched tissues from known positives and negatives and hybridization with digoxigenin-labeled sense RNA. Slides were then incubated with antibodies listed in Table 2, and imaged by confocal microscopy, as outlined above.

Results

Histopathology findings

As indicated in Table 1, of the 22 animals euthanized with clinical AIDS, eleven had SIVE characterized by perivascular aggregates of mononuclear cells and multinucleated giant cells along with variable areas of gliosis as described previously [40–43]. The SIVE lesions were observed in both gray and white matter of brain, but predominantly in white matter. The remaining eleven animals without SIVE lesions had no significant neuropathologic abnormalities in the CNS. Regardless of the presence of SIVE, all 22 SIV infected animals had AIDS defining pathologies such as profound CD4+ T cell depletion and multiple opportunistic infections and generalized lymphoid depletion. The uninfected control animals were not terminal cases, and so no histologic data was available for this group.

Outside of the brain, chronic inflammatory lesions characterized by lymphoplasmacytic infiltrates mixed with variable numbers of syncytial giant cells were noted with equal frequency and intensity for both study groups in lung, liver, heart, liver, skeletal muscle, salivary gland and trachea. Slight group differences were identified in some tissues. Chronic inflammation in kidney and colon was more frequent in the SIVE group (9/11) compared with the SIVnoE group (6/11). The range of intensity of inflammation was greater in the kidney (2–4 vs 1–2) but comparable in the colon. Also, more SIVE animals had inflammation in the skin (2/11) compared with the SIVnoE animals (0) and around the sciatic nerves (4/11 vs 2/11). In contrast, more non-SIVE animals had inflammatory lesions of the small intestine (5/11) than the SIVE animals (2/11) and had infrequent lesions in the reproductive tissues (prostate, vagina; 2/11) compared with no lesions in the SIVE animals. Morphologic evaluation of lymphoid tissues suggested similar degrees of hyperplasia were present in lymph nodes, spleen, and bone marrow while generalized depletion of lymphoid

tissues was slightly more frequent in the non-SIVE group (4/11) compared with the SIVE group (2/11).

Elevations of serum S100β are associated with SIVE

To determine if animals with encephalitis had increased levels of S100β in serum, we performed an ELISA for S100β in all animals in the study. Serum was obtained from blood drawn at the time of euthanasia. Figure 1A demonstrates the levels of S100β in serum of SIV-infected animals with or without encephalitis, and uninfected controls. The animals with SIVE had higher serum levels of S100β [mean, 1.73 ng/ml (range, 0.19–4.40 ng/ml)] than that of SIV infected animals without encephalitis [mean, 0.31 ng/ml (range, 0.09–1.30 ng/ml)] and uninfected control animals [mean, 0.44 ng/ml (range, 0.16–.92 ng/ml)] (ANOVA, $p = 0.001$). Fisher's Exact Test demonstrated that animals with S100β values of greater than 1ng/ml could be predicted to have encephalitis, and animals with values less than 1ng/ml to be unlikely to have encephalitis ($p<0.0001$).

We plotted the number of lesions/ mm^2 (shown in Table 1) against the level of S100β in serum for all SIV-infected animals on this study (Figure 1B). The correlation between the level of S100β in serum and the number of lesions/ mm^2 was analyzed using Pearson correlation (correlation= 0.527, $p= 0.002$). Thus, animals with SIVE had significantly higher S100β levels compared to animals without encephalitis. However, analyses of SIVE animals in isolation revealed that there was no significant correlation between S100β levels in serum and number of lesions / mm^2.

Correlation between weight loss, diagnosis of SIVE, and serum levels of S100β protein

It has previously been shown in rats that rapid weight loss was associated with increased S100β in serum [44]. To eliminate this possibility as a confound, we examined weight loss in relation to S100β levels (Figure 2A, Pearson Correlation= 0.083, $p= 0.65$), and lesions/ mm^2 (Pearson Correlation= 0.13, $p= 0.47$, not shown) Our data show that S100β levels were not significantly correlated with weight change, or density of inflammatory lesions. Therefore, elevated S100β was confirmed to be specific to SIVE animals, and not an epiphenomenon of terminal SIV infection.

S100β protein levels are not correlated with peak or terminal viral load

To rule out increased S100β protein in serum with other parameters of SIV infection we performed statistical analyses to determine if there was a correlation with peak (Figure 2B) or terminal (Figure 2C) viral load. Viral load data was used from all animals that had had viral load testing performed at the time of necropsy. Our data show that S100β levels were not significantly correlated with these parameters ($p>0.05$ in both cases), further confirming that S100β is specific to SIVE animals.

To confirm that the S100β levels in serum were specific, and not part of a generalized inflammatory response, we measured levels of CRP, IL-6 and CCL2. Levels of CRP, IL-6 and CCL2 in animals with SIVE were not significantly different from non-SIVE animals. Although, CRP values were significantly higher in non-SIVE animals than controls ($p<0.001$), this was not true in SIVE animals. In contrast, IL-6 was significantly elevated in both groups of SIV-infected macaques, regardless of encephalitic status. However, there was no significant difference between IL-6 levels between SIVE and SIVnoE animals (Figure 2E). Levels of CCL2 were not significantly different in any of the three groups (Figure 2F). There was no correlation between levels of S100β and CRP ($p=0.8044$), IL-6 ($p=0.7791$) or CCL2 ($p=0.5038$).

Increased serum levels of S100β protein is associated with loss of tight junction protein ZO-1 in SIVE lesions

We sought to determine if increased S100β protein in serum was associated with loss of the critical tight junction protein ZO-1 on brain microvessels and the presence of SIV-infected cells. This was done by combining *in situ* hybridization for SIV RNA (to determine productively infected cells) and semi-quantitative immunofluorescence for ZO-1. Animals without elevated S100β had the anticipated linear pattern of ZO-1 expression along the lengths of the microvessels (Figure 3A, see inset for details. Scale bars represent 50μm in each image). In animals with increased S100β, there was markedly decreased expression of ZO-1 protein (green) around lesions with numerous SIV-infected cells (Figures 3 B&C). These productively-infected cells were predominately CD68 positive macrophages in agreement with previously published work [14, 45] (not shown). Represented graphically, control animals had high ZO-1 levels combined with low S100β (Figure 3D). SIV infected animals without encephalitis were not significantly different from the controls. Animals with SIVE had significantly decreased ZO-1 expression compared with each of control or SIV without encephalitis ($p=0.0008$, Kruskal-Wallis test).

Loss of ZO-1 and elevated serum S100β is correlated with leakage of serum proteins into the brain parenchyma

Finally, we sought to determine if the elevations in S100β and loss of ZO-1 expression was associated with leakage of serum proteins into the brain parenchyma. To do this, we performed multilabel confocal microscopy to examine ZO-1 and plasma fibrinogen in the CNS of these animals. Fibrinogen in the parenchyma has previously been shown to be a marker of breakdown of the BBB in encephalitis [46]. In control macaques, or macaques without encephalitis, very little if any fibrinogen (green) was detected in brain parenchyma (Figure 4A) consistent with the results of others [46]. In macaques with SIVE, the deposition of fibrinogen coincided with diminished ZO-1 (red) protein expression and a loss of the linear pattern of ZO-1 expression seen in animals without SIVE.

The pattern of fibrinogen deposition varied from focal intense aggregates (Figure 4B) in areas without ZO-1 expression to more diffuse expression around vessels (Figure 4C). The latter was primarily found around the larger vessels. It is possible that this is because these larger vessels have their own capillary supply. The leakage may be more readily visible because of the density of leaky small vessels around these larger vessels. These results are summarized in Table 3. This leakage of fibrinogen into the parenchyma was shown to be significantly increased in animals with encephalitis ($p<0.0001$, Chi-squared test).

Discussion

In order to determine if it is possible to predict encephalitis in macaques infected with SIV, we correlated the levels of S100β protein in serum with the degree of encephalitis in terminal SIV infection. In addition, the tight junction protein ZO-1 was found to be diminished in those animals with the highest degree of encephalitis/levels of S100β protein, and with leakage of serum proteins into the parenchyma. Finally, we showed that this increased S100β protein expression was not due to extracerebral sources as evidenced by lack of significant correlation of loss of weight with increased S100β protein in serum. Combined, those animals with increased S100β in serum at terminal AIDS also had histological evidence of SIVE, diminished ZO-1 and fibrinogen leakage into parenchyma.

Although disruption of the BBB is present in terminal AIDS, it is not yet known when it begins. BBB disruption in other conditions has been demonstrated *in vivo* using S100β protein in serum [31]. Using this technique, it may be possible to determine if a subject has

encephalitis in the earliest stages of neuroAIDS. Elucidating the molecular basis for the alterations observed in endothelial cells during the earliest stages of neuroAIDS would allow one to begin to devise strategies to inhibit this BBB disruption and the associated neurological complications.

In an attempt to quantify leakage of parenchymal protein into plasma (and therefore serum), the S100β ELISA was used to approximate disruption of the BBB at terminal disease [32–34]. The data showed variable levels of S100β protein in the serum samples assayed (Figure 1A), indicating differences in the permeability of the BBB of the 22 terminal AIDS animals included in this study. It should be noted that these serum samples were obtained at time of euthanasia.

It is a matter of record that there is lentiviral infection of brain tissues during early infection [3, 15, 47]. MCP-1/CCL2 protein can be found in CSF prior to onset of encephalitis [48] and S100β has been correlated in CSF with severity of AIDS dementia complex [49], this procedure is too invasive to be practical with human patients. We propose S100β protein in serum to be more practical than the above methods, and is less invasive than previous *in vivo* measures of permeability [50].

S100β is a short lived protein in serum, with a half-life of approximately 25 minutes [51]. Thus, any S100β measured in serum must have been released recently into the bloodstream. It is known that animals infected with SIV lose considerable body weight in terminal AIDS [52]. It is also a matter of record that fasting animals have increased S100β in serum, mainly from extracerebral sources [44]. S100β has also been reported to be located in adipose cells [53], possibly within pluripotent stem cells that can differentiate into Schwann cells or neurons [54]. It has been argued previously that S100β protein in serum of cardiac bypass patients can be derived from non-brain tissues [55, 56] rather than being necessarily from cerebral derived sources. However, the statistical correlation between encephalitic animals and levels of S100β protein, combined with a lack of correlation between increased S100β and weight loss leads one to conclude that S100β protein in serum can legitimately be used as a marker for BBB breakdown, and thus SIVE. Other inflammatory proteins measured - CRP, IL-6, and CCL2 - taken individually, or together, could not be correlated with the presence of SIVE.

Other groups have recently shown increased fibrinogen leakage into parenchymal tissues around induced lesions [46]. Our studies also show that this protein is found in brains of animals with increased S100β protein expression. Concomitant with this, there is also decreased expression of the tight junction protein ZO-1 in those animals with increased S100β protein. Loss of this protein has been shown previously to be indicative of loss of BBB integrity in HIV and SIV encephalitis [20, 23, 24, 37].

Thus, increased S100β protein in serum of rhesus macaques infected with SIVmac239/251 is a highly efficient and practical method of determining encephalitic status. It correlates well with decreased ZO-1 expression and leakage of serum proteins into the parenchyma. Although, almost all animals lost weight before being euthanized, weight loss was not a significant factor in the increased S100β protein in serum. We propose that S100β in serum to be a useful indicator for SIV/HIV encephalitis premortem.

Acknowledgments

This work was supported by PHS grants RR00164, MH077544 (AGM), Louisiana Board of Regents Fellowship LEQSF(2007-2012)-GF15 (NAR). We thank the faculty and staff of the PDQC, clinical and confocal cores at TNPRC.

References

1. Lackner AA, Vogel P, Ramos RA, Kluge JD, Marthas M. Early events in tissues during infection with pathogenic (SIVmac239) and nonpathogenic (SIVmac1A11) molecular clones of simian immunodeficiency virus. Am J Pathol. 1994; 145:428–439. [PubMed: 8053500]
2. Davis LE, Hjelle BL, Miller VE, Palmer DL, Llewellyn AL, Merlin TL, Young SA, Mills RG, Wachsman W, Wiley CA. Early viral brain invasion in iatrogenic human immunodeficiency virus infection. Neurology. 1992; 42:1736–1739. [PubMed: 1513462]
3. Stephens EB, Singh DK, Kohler ME, Jackson M, Pacyniak E, Berman NE. The primary phase of infection by pathogenic simian-human immunodeficiency virus results in disruption of the blood-brain barrier. AIDS Res Hum Retroviruses. 2003 Oct.19:837–846. [PubMed: 14585215]
4. Sasseville VG, Lane JH, Walsh D, Ringler DJ, Lackner AA. VCAM-1 expression and leukocyte trafficking to the CNS occur early in infection with pathogenic isolates of SIV. J Med Primatol. 1995; 24:123–131. [PubMed: 8751051]
5. Annunziata P. Blood-brain barrier changes during invasion of the central nervous system by HIV-1. Old and new insights into the mechanism. J Neurol. 2003 Aug.250:901–906. [PubMed: 12928906]
6. Zink MC, Spelman JP, Robinson RB, Clements JE. SIV infection of macaques--modeling the progression to AIDS dementia. J Neurovirol. 1998; 4:249–259. [PubMed: 9639068]
7. Little SJ, McLean AR, Spina CA, Richman DD, Havlir DV. Viral dynamics of acute HIV-1 infection. J Exp Med. 1999; 190:841–850. [PubMed: 10499922]
8. Gorry PR, Ong C, Thorpe J, Bannwarth S, Thompson KA, Gatignol A, Vesselingh SL, Purcell DF. Astrocyte infection by HIV-1: mechanisms of restricted virus replication, and role in the pathogenesis of HIV-1-associated dementia. Curr HIV Res. 2003 Oct.1:463–473. [PubMed: 15049431]
9. Bissel SJ, Wiley CA. Human immunodeficiency virus infection of the brain: pitfalls in evaluating infected/affected cell populations. Brain Pathol. 2004 Jan.14:97–108. [PubMed: 14997942]
10. Ryzhova EV, Crino P, Shawver L, Westmoreland SV, Lackner AA, Gonzalez-Scarano F. Simian immunodeficiency virus encephalitis: analysis of envelope sequences from individual brain multinucleated giant cells and tissue samples. Virology. 2002 May 25.297:57–67. [PubMed: 12083836]
11. Liu Y, Liu H, Kim BO, Gattone VH, Li J, Nath A, Blum J, He JJ. CD4-independent infection of astrocytes by human immunodeficiency virus type 1: requirement for the human mannose receptor. J Virol. 2004 Apr.78:4120–4133. [PubMed: 15047828]
12. Brack-Werner R. Astrocytes: HIV cellular reservoirs and important participants in neuropathogenesis. Aids. 1999 Jan 14.13:1–22. [PubMed: 10207540]
13. Trillo-Pazos G, Diamanturos A, Rislove L, Menza T, Chao W, Belem P, Sadiq S, Morgello S, Sharer L, Volsky DJ. Detection of HIV-1 DNA in microglia/macrophages, astrocytes and neurons isolated from brain tissue with HIV-1 encephalitis by laser capture microdissection. Brain Pathol. 2003 Apr.13:144–154. [PubMed: 12744468]
14. Williams KC, Corey S, Westmoreland SV, Pauley D, Knight H, deBakker C, Alvarez X, Lackner AA. Perivascular Macrophages Are the Primary Cell Type Productively Infected by Simian Immunodeficiency Virus in the Brains of Macaques. Implications for the neuropathogenesis of aids. J Exp Med. 2001; 193:905–916. [PubMed: 11304551]
15. Fischer-Smith T, Croul S, Sverstiuk AE, Capini C, L'Heureux D, Regulier EG, Richardson MW, Amini S, Morgello S, Khalili K, Rappaport J. CNS invasion by CD14+/CD16+ peripheral blood-derived monocytes in HIV dementia: perivascular accumulation and reservoir of HIV infection. J Neurovirol. 2001; 7:528–541. [PubMed: 11704885]
16. Nath A, Conant K, Chen P, Scott C, Major EO. Transient exposure to HIV-1 tat protein results in cytokine production in macrophages and astrocytes. Journal of biological chemistry. 1999; 274:17098–17102. [PubMed: 10358063]
17. Tyor WR, Glass JD, Griffin JW, Becker PS, McArthur JC, Bezman L, Griffin DE. Cytokine expression in the brain during the acquired immunodeficiency syndrome. Ann Neurol. 1992; 31:349–360. [PubMed: 1586135]

18. Persidsky Y, Ghorpade A, Rasmussen J, Limoges J, Liu XJ, Stins M, Fiala M, Way D, Kim KS, Witte MH, Weinand M, Carhart L, Gendelman HE. Microglial and astrocyte chemokines regulate monocyte migration through the blood-brain barrier in human immunodeficiency virus-1 encephalitis. Am J Pathol. 1999; 155:1599–1611. [PubMed: 10550317]
19. Persidsky Y, Zheng J, Miller D, Gendelman HE. Mononuclear phagocytes mediate blood-brain barrier compromise and neuronal injury during HIV-1-associated dementia. J Leukoc Biol. 2000 Sep.68:413–422. [PubMed: 10985259]
20. Dallasta LM, Pisarov LA, Esplen JE, Werley JV, Moses AV, Nelson JA, Achim CL. Blood-brain barrier tight junction disruption in human immunodeficiency virus-1 encephalitis. Am J Pathol. 1999; 155:1915–1927. [PubMed: 10595922]
21. Persidsky Y, Stins M, Way D, Witte MH, Weinand M, Kim KS, Bock P, Gendelman HE, Fiala M. A model for monocyte migration through the blood-brain barrier during HIV-1 encephalitis. J Immunol. 1997; 158:3499–3510. [PubMed: 9120312]
22. Moses AV, Nelson JA. HIV infection of human brain capillary endothelial cells--implications for AIDS dementia. Adv Neuroimmunol. 1994; 4:239–247. [PubMed: 7533040]
23. Boven LA, Middel J, Verhoef J, De Groot CJ, Nottet HS. Monocyte infiltration is highly associated with loss of the tight junction protein zonula occludens in HIV-1-associated dementia. Neuropathol Appl Neurobiol. 2000; 26:356–360. [PubMed: 10931369]
24. Luabeya MK, Dallasta LM, Achim CL, Pauza CD, Hamilton RL. Blood-brain barrier disruption in simian immunodeficiency virus encephalitis. Neuropathol Appl Neurobiol. 2000; 26:454–462. [PubMed: 11054186]
25. Andras IE, Pu H, Deli MA, Nath A, Hennig B, Toborek M. HIV-1 Tat protein alters tight junction protein expression and distribution in cultured brain endothelial cells. J Neurosci Res. 2003 Oct 15.74:255–265. [PubMed: 14515355]
26. Kanmogne GD, Primeaux C, Grammas P. HIV-1 gp120 proteins alter tight junction protein expression and brain endothelial cell permeability: implications for the pathogenesis of HIV-associated dementia. J Neuropathol Exp Neurol. 2005 Jun.64:498–505. [PubMed: 15977641]
27. Kanmogne GD, Schall K, Leibhart J, Knipe B, Gendelman HE, Persidsky Y. HIV-1 gp120 compromises blood-brain barrier integrity and enhances monocyte migration across blood-brain barrier: implication for viral neuropathogenesis. J Cereb Blood Flow Metab. 2007 Jan.27:123–134. [PubMed: 16685256]
28. MacLean AG, Rasmussen TA, Bieniemy DN, Alvarez X, Lackner AA. SIV-induced activation of the blood-brain barrier requires cell-associated virus and is not restricted to endothelial cell activation. J Med Primatol. 2004 Oct.33:236–242. [PubMed: 15525324]
29. Persidsky Y. Model systems for studies of leukocyte migration across the blood - brain barrier. J Neurovirol. 1999; 5:579–590. [PubMed: 10602399]
30. Ellis EF, Willoughby KA, Sparks SA, Chen T. S100B protein is released from rat neonatal neurons, astrocytes, and microglia by in vitro trauma and anti-S100 increases trauma-induced delayed neuronal injury and negates the protective effect of exogenous S100B on neurons. J Neurochem. 2007 Jun.101:1463–1470. [PubMed: 17403138]
31. Marchi N, Cavaglia M, Fazio V, Bhudia S, Hallene K, Janigro D. Peripheral markers of blood-brain barrier damage. Clin Chim Acta. 2004 Apr.342:1–12. [PubMed: 15026262]
32. Fazio V, Bhudia SK, Marchi N, Aumayr B, Janigro D. Peripheral detection of S100beta during cardiothoracic surgery: what are we really measuring? Ann Thorac Surg. 2004 Jul.78:46–52. discussion -3. [PubMed: 15223400]
33. Kanner AA, Marchi N, Fazio V, Mayberg MR, Koltz MT, Siomin V, Stevens GH, Masaryk T, Ayumar B, Vogelbaum MA, Barnett GH, Janigro D. Serum S100beta: a noninvasive marker of blood-brain barrier function and brain lesions. Cancer. 2003 Jun 1.97:2806–2813. [PubMed: 12767094]
34. Kapural M, Krizanac-Bengez L, Barnett G, Perl J, Masaryk T, Apollo D, Rasmussen P, Mayberg MR, Janigro D. Serum S-100beta as a possible marker of blood-brain barrier disruption. Brain Res. 2002 Jun 14.940:102–104. [PubMed: 12020881]

35. Marchi N, Rasmussen P, Kapural M, Fazio V, Kight K, Mayberg MR, Kanner A, Ayumar B, Albensi B, Cavaglia M, Janigro D. Peripheral markers of brain damage and blood-brain barrier dysfunction. Restor Neurol Neurosci. 2003; 21:109–121. [PubMed: 14530574]
36. Sen J, Belli A. S100B in neuropathologic states: the CRP of the brain? J Neurosci Res. 2007 May 15.85:1373–1380. [PubMed: 17348038]
37. MacLean AG, Belenchia GE, Bieniemy DN, Moroney-Rasmussen TA, Lackner AA. Simian immunodeficiency virus disrupts extended lengths of the blood--brain barrier. J Med Primatol. 2005 Oct.34:237–242. [PubMed: 16128918]
38. Howard, V.; Reed, MG. Unbiased stereology : three-dimensional measurement in microscopy. New York: Springer; 1998.
39. Borda JT, Alvarez X, Mohan M, Hasegawa A, Bernardino A, Jean S, Aye P, Lackner AA. CD163, a Marker of Perivascular Macrophages, Is Up-Regulated by Microglia in Simian Immunodeficiency Virus Encephalitis after Haptoglobin-Hemoglobin Complex Stimulation and Is Suggestive of Breakdown of the Blood-Brain Barrier. Am J Pathol. 2008 Mar.172:725–737. [PubMed: 18276779]
40. Williams KC, Corey S, Westmoreland SV, Pauley D, Knight H, deBakker C, Alvarez X, Lackner AA. Perivascular macrophages are the primary cell type productively infected by simian immunodeficiency virus in the brains of macaques: implications for the neuropathogenesis of AIDS. J Exp Med. 2001 Apr 16.193:905–915. [PubMed: 11304551]
41. Chakrabarti L, Hurtrel M, Maire M, Vazeux R, Dormont D, Montagnier L, Hurtrel B. Early viral replication in the brain of SIV-infected rhesus monkeys. Am J Pathol. 1991; 139:1273–1280. [PubMed: 1750503]
42. Smith MO, Heyes MP, Lackner AA. Early intrathecal events in rhesus macaques (Macaca mulatta) infected with pathogenic or nonpathogenic molecular clones of simian immunodeficiency virus. Lab Invest. 1995 May.72:547–558. [PubMed: 7745949]
43. Lackner, AA. Pathology of simian immunodeficiency virus induced disease. In: Desrosiers, RC.; Letvin, N., editors. Current Topics in Microbiology and Immunology: Simian Immunodeficiency Virus. Berlin: Springer Verlag; 1994. p. 35-64.
44. Netto CB, Conte S, Leite MC, Pires C, Martins TL, Vidal P, Benfato MS, Giugliani R, Goncalves CA. Serum S100B protein is increased in fasting rats. Arch Med Res. 2006 Jul.37:683–686. [PubMed: 16740441]
45. Sasseville VG, Lackner AA. Neuropathogenesis of simian immunodeficiency virus infection in macaque monkeys. J Neurovirol. 1997; 3:1–9. [PubMed: 9147816]
46. Willis CL, Leach L, Clarke GJ, Nolan CC, Ray DE. Reversible disruption of tight junction complexes in the rat blood-brain barrier, following transitory focal astrocyte loss. Glia. 2004 Oct. 48:1–13. [PubMed: 15326610]
47. Lane JH, Sasseville VG, Smith MO, Vogel P, Pauley DR, Heyes MP, Lackner AA. Neuroinvasion by simian immunodeficiency virus coincides with increased numbers of perivascular macrophages/microglia and intrathecal immune activation. J Neurovirol. 1996; 2:423–432. [PubMed: 8972425]
48. Zink MC, Coleman GD, Mankowski JL, Adams RJ, Tarwater PM, Fox K, Clements JE. Increased macrophage chemoattractant protein-1 in cerebrospinal fluid precedes and predicts simian immunodeficiency virus encephalitis. J Infect Dis. 2001; 184:1015–1021. [PubMed: 11574916]
49. Pemberton LA, Brew BJ. Cerebrospinal fluid S-100beta and its relationship with AIDS dementia complex. J Clin Virol. 2001 Oct.22:249–253. [PubMed: 11564589]
50. Ivey NS, Martin EN Jr, Scheld WM, Nathan BR. A new method for measuring blood-brain barrier permeability demonstrated with Europium-bound albumin during experimental lipopolysaccharide (LPS) induced meningitis in the rat. J Neurosci Methods. 2005 Mar 15.142:91–95. [PubMed: 15652621]
51. Jonsson H, Johnsson P, Hoglund P, Alling C, Blomquist S. Elimination of S100B and renal function after cardiac surgery. J Cardiothorac Vasc Anesth. 2000 Dec.14:698–701. [PubMed: 11139112]

52. Baskin GB, Murphey-Corb M, Watson EA, Martin LN. Necropsy findings in rhesus monkeys experimentally infected with cultured simian immunodeficiency virus (SIV)/delta. Vet Pathol. 1988; 25:456–467. [PubMed: 2850650]

53. Bannerman PG, Mirsky R, Jessen KR. Establishment and properties of separate cultures of enteric neurons and enteric glia. Brain Res. 1988 Feb 2.440:99–108. [PubMed: 2896046]

54. Kingham PJ, Kalbermatten DF, Mahay D, Armstrong SJ, Wiberg M, Terenghi G. Adipose-derived stem cells differentiate into a Schwann cell phenotype and promote neurite outgrowth in vitro. Exp Neurol. 2007 Oct.207:267–274. [PubMed: 17761164]

55. Kleine TO, Benes L, Zofel P. Studies of the brain specificity of S100B and neuron-specific enolase (NSE) in blood serum of acute care patients. Brain Res Bull. 2003 Aug 15.61:265–279. [PubMed: 12909297]

56. Anderson RE, Hansson LO, Nilsson O, Liska J, Settergren G, Vaage J. Increase in serum S100A1-B and S100BB during cardiac surgery arises from extracerebral sources. Ann Thorac Surg. 2001 May.71:1512–1517. [PubMed: 11383792]

1A

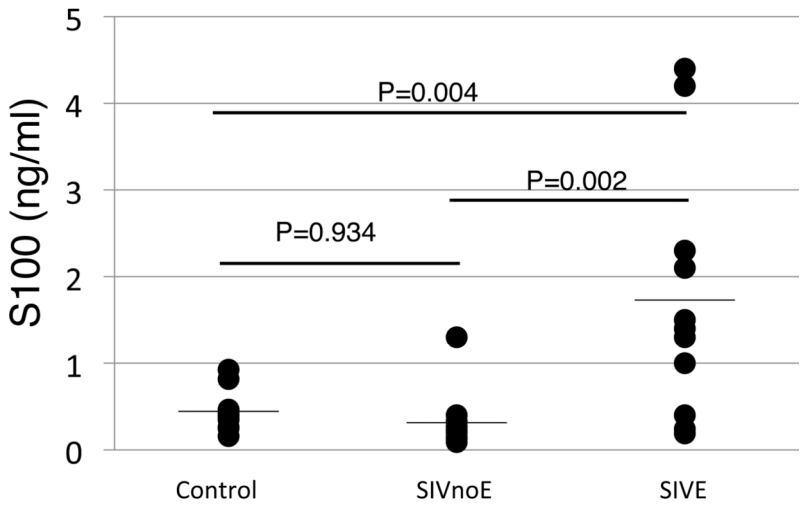

1B

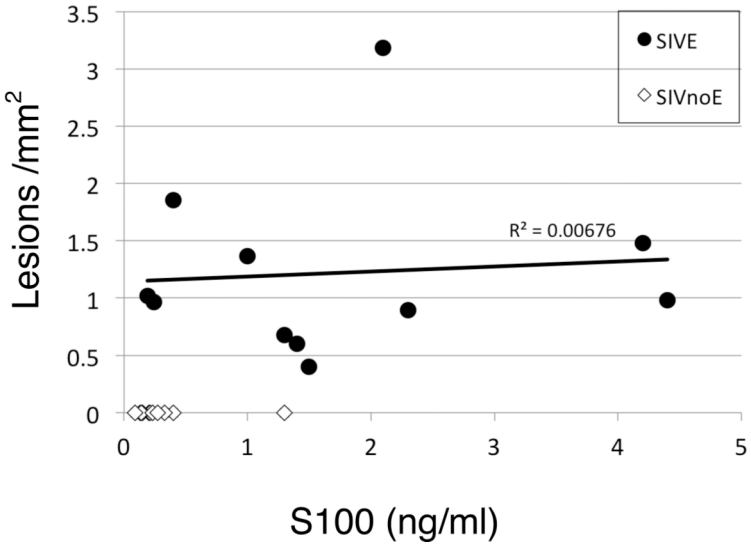

Figure 1. Increased expression of S100β in encephalitic animals

Those animals with encephalitis had elevated serum levels of S100β protein (A) compared with animals without evidence of encephalitis, and noninfected control animals. Graphs represent means of duplicate samples. When lesions/mm^2 were plotted against S100β ELISA scores, it was apparent that animals with encephalitic lesions had elevated S100β (B, Pearson correlation= 0.527, p=0.002).

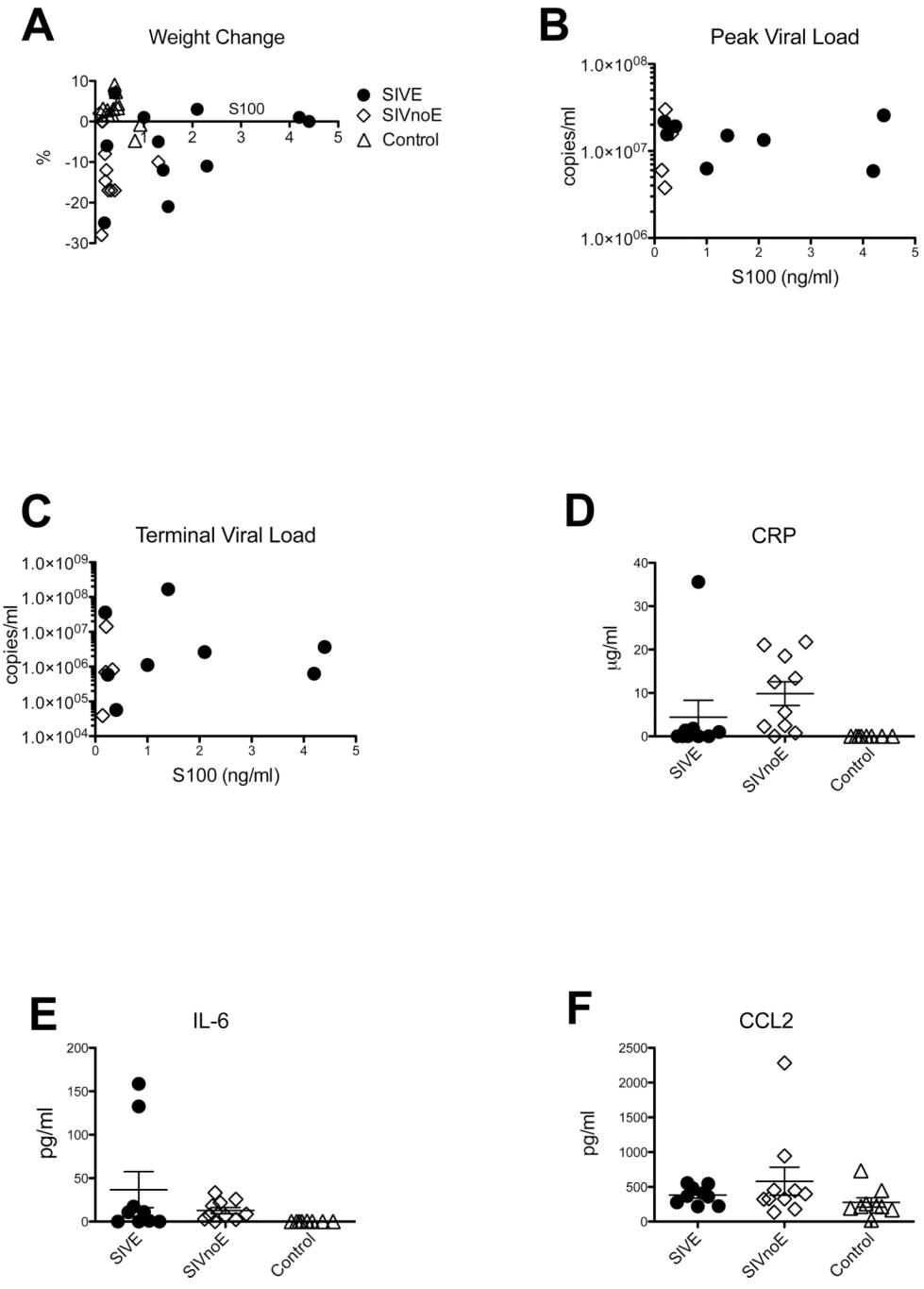

Figure 2. Correlation of weight loss and increased S100β levels in serum

To determine if increased S100β in serum correlated with loss of body mass, we plotted the body mass as percent increase / decrease in the month before necropsy (A). When percentage change in mass is plotted against S100β concentration, there is no significant difference between animals with encephalitis (black circles), and those without encephalitis (open diamonds) or control animals (open triangles) ($p=0.646$). There was also no correlation of S100β concentration with either peak (B) or terminal (C) viral load. CRP values (D) for encephalitic animals were not significantly different from those without encephalitis ($p>0.05$), or control animals ($p>0.05$). Levels of IL-6 (E) were significantly higher in SIV infected animals compared with controls ($p=0.0053$), but were not

significantly different between encephalitic and non-encephalitic animals ($p>0.05$). No significant difference in MCP-1/CCL2 expression was found in any group of animals CCL2 (F) levels ($p>0.05$).

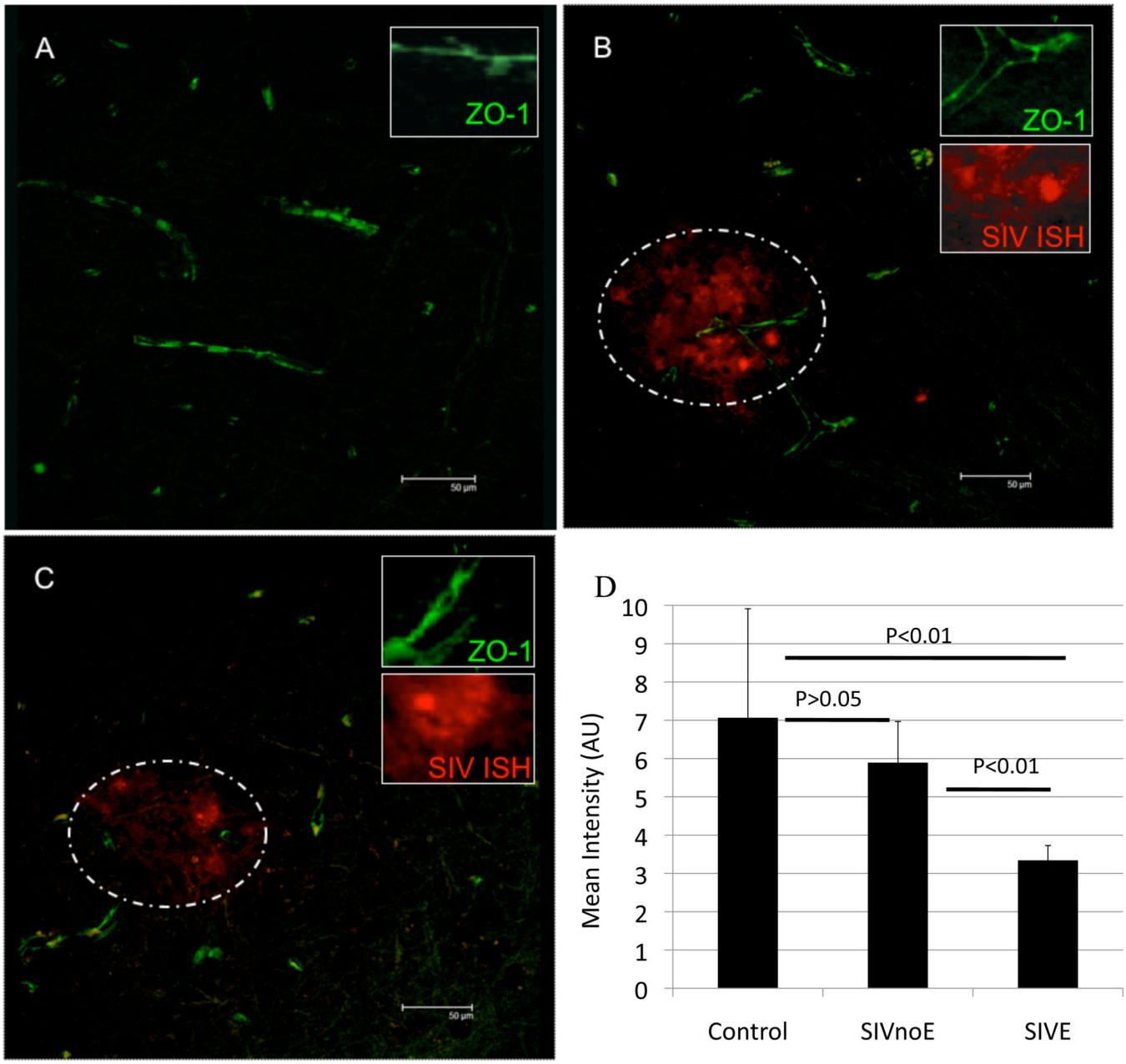

Figure 3. Expression of endothelial tight junction proteins in macaques with or without SIVE

To determine if the animals with elevated serum levels of S100β also had decreased levels of tight junction protein expression we examined expression of ZO-1 by immunofluorescence and performed *in situ* hybridization for viral RNA. Animals without SIVE (A) had a continuous staining pattern of ZO-1 labeling along the vessel (green). Within encephalitic lesions, there was loss of the characteristic linear ZO1 expression (B). This was particularly apparent in the vicinity of SIV-infected cells (red) detected by *in situ* hybridization. Lesions are outlined with dotted line. The degree of loss of ZO-1 was variable with some vessels (C) nearly devoid of ZO-1. Calculated expression of ZO-1 in capillaries from control macaques or macaques infected with SIV, but without encephalitis, were not significantly different from each other (D). Animals with SIVE had significantly diminished

expression of ZO-1 compared with either SIV-infected animals without encephalitis ($p<0.01$) or controls ($p<0.01$).

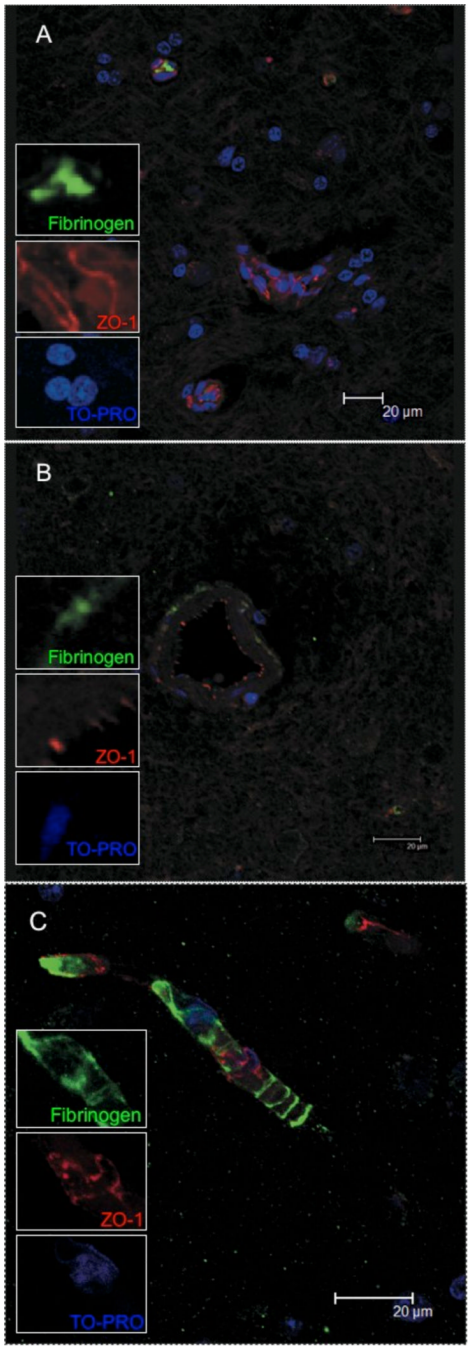

Figure 4. Leakage of serum proteins into parenchyma

To examine the integrity of brain microvessels we looked for fibrinogen in the brain parenchyma. Control animals had little evidence of fibrinogen (A, green) in the parenchyma. It was noted that fibrinogen was contained within a vessel (top left and green inset). In contrast, encephalitic animals showed fibrinogen around vessels, indicating leakage from vessels (B). This leakage was significantly different between groups $p<0.0001$). Further, the ZO-1 labeling was quite punctate and not continuous as seen on vessels from normal animals (figure 3A and 4A). Fibrinogen (green) could be seen around vessels in areas where there were gaps in endothelial labeling for ZO-1 (red) (C).

Table 1

Animals, Inoculum, Neuropathologic diagnoses and lesions.

	Animal	Inoculum	Major Neuropathologic Diagnoses	Days Post-Infection	Lesions/ mm^2
SIV encephalitis	AV89	SIVmac239	SIVE	888	0.895
	BI63	SIVmac251	SIVE	149	0.399
	BR06	SIVmac251	SIVE	92	0.676
	CF52	SIVmac239	SIVE	483	1.368
	CL77	SIVmac239	SIVE	787	1.853
	CT83	SIVmac239	SIVE	1062	1.475
	DD95	SIVmac239	SIVE	468	0.983
	DE68	SIVmac239	SIVE	70	0.603
	DE99	SIVmac239	SIVE	119	1.019
	DP30	SIVmac251	SIVE	399	3.183
	EN84	SIVmac239	SIVE	569	0.963
SIV, no encephalitis	BA25	SIVmac239	NSL	862	0
	BE65	SIVmac251	NSL	1087	0
	CC47	SIVmac251	NSL	680	0
	DD44	SIVmac251	NSL	507	0
	DE57	SIVmac251	NSL	245	0
	DG96	SIVmac239	NSL	147	0
	EE54	SIVmac239	NSL	364	0
	EI69	SIVmac251	NSL	89	0
	EI70	SIVmac251	NSL	57	0
	P045	SIVmac239	NSL	1140	0
	T687	SIVmac239	NSL	546	0
Uninfected	DE95	n/a	still alive	n/a	
	FD38	n/a	still alive	n/a	
	FV11	n/a	still alive	n/a	
	FV53	n/a	still alive	n/a	

	Animal	Inoculum	Major Neuropathologic Diagnoses	Days Post-Infection	Lesions/mm^2
	GH59	n/a	still alive	n/a	
	GI43	n/a	still alive	n/a	
	GI51	n/a	still alive	n/a	
	GK37	n/a	still alive	n/a	
	GM61	n/a	still alive	n/a	
	GP19	n/a	still alive	n/a	
	HD92	n/a	still alive	n/a	

Table 2

Antibodies, dilutions and sources used in studies.

Antibody	Source	Species	Dilution
Fibrinogen	Dako	Rabbit	1/100
ZO-1	Zymed	Mouse	6/100
Secondary fluorescent antibodies	Molecular Probes	Rabbit/mouse IgG	1/1000

Table 3

Summary of findings.

	S100β	Neurological lesions	ZO-1 expression	Fibrinogen in tissues
Uninfected	Below 1ng/ml	None	Normal, linear	No
Infected, no encephalitis	Below 1ng/ml	None	Normal, linear	No
SIV encephalitis	Above 1ng/ml	Yes	Punctate, or missing	Yes